

Maurizio Fantini * and Silvio Davolio
ISAO-CNR, Bologna, Italy

1 INTRODUCTION

The interaction of a baroclinic wave with localized topography is studied in a quasi geostrophic Eady model in which a basic state, constituted of a two-dimensional finite amplitude neutral wave (hereafter referred to as the 'primary' wave) superposed on the uniformly sheared zonal wind, is made to interact with a linearized mountain. The orographic perturbations thus produced change behavior according to the amplitude of the primary wave: they are slightly deformed Eady waves when the primary wave amplitude is small, and resemble instead frontal waves in the large amplitude case. The latter case displays an 'absolute instability' behavior, i.e. the packet generated by the mountain grows in place so that at a fixed location one could observe an exponentially growing disturbance. In the opposite case, which obtains when the amplitude of the primary wave is small (including zero, i.e. the classic Eady model), the orographic wave packet is advected by the mean zonal wind and at any fixed location the perturbation will asymptotically vanish. A review of the concepts of absolute and convective instability as they apply to baroclinic flows is given in Pierrehumbert and Swanson (1995).

2 NORMAL MODES

In order to understand the characteristics of the orographically generated disturbances, the instability of a finite amplitude two-dimensional neutral Eady wave is studied by long time integrations of a quasi-geostrophic numerical model, initialized with a random θ perturbation at the lower boundary, which let the most unstable normal mode appear. As primary wave we selected the lower neutral Eady mode, which has maximum amplitude at the surface and a phase speed lower than the midlevel wind. Fig.1 summarizes the eigenvalues (growth rate and phase speed) for the most unstable mode when the amplitude of the primary wave is changed, while Figs 2 and 3 show the surface geopotential of the most unstable perturbation when the primary wave is 25 mb and 1 mb deep, respectively.

In the case of small amplitude of the primary wave

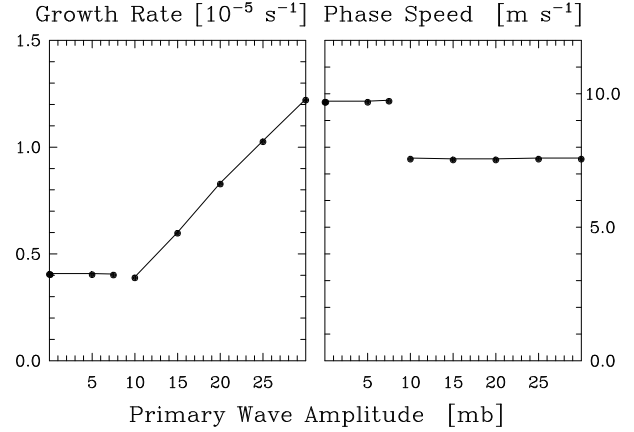


Figure 1: Growth rate (left panel) and phase speed (right panel) of the most unstable mode growing on uniform zonal shear plus finite amplitude Eady wave, vs amplitude of the Eady wave. The left (small Eady amplitude) branch of the curves represents modes like the one displayed in Fig.3 below, while the right branch refers to the modes of Fig.2. The break in between is a range of parameters in which the two types of modes compete with nearly the same growth rate, and the numerical simulations fail to distinguish between them.

the growth rate does not differ sensibly from the classic Eady results. The values shown in Fig.1 are obtained for a 3,500 km long primary wave, 20 m/s vertical shear of the zonal wind, and a uniform static stability of $1.5 \times 10^{-2} \text{ s}^{-1}$, so that the Rossby radius of deformation is 1,500 km. The phase speed is the same, within the limits of a numerical estimate, as in the case of zero amplitude, i.e. the mean wind at midlevel.

Figure 3 gives the surface geopotential for the most unstable mode in the case of a primary wave 1 mb deep. The domain shown comprises 8 wavelengths of the primary wave, and the wavelength of the perturbation shown can be evaluated at 5,600 km. As in the case of no primary wave the most unstable mode is the one with infinite meridional extent (at the time shown the perturbation has not fully reached the normal structure).

The rightmost part of the curves displayed in Fig.1 refers to the most unstable perturbation in cases of a primary wave of large amplitude, whose spatial pattern is shown in Fig.2. The growth rate is seen to grow

* Corresponding author address: Maurizio Fantini, ISAO-CNR, via Gobetti 101, Bologna 40129, Italy; email: M.Fantini@isao.bo.cnr.it

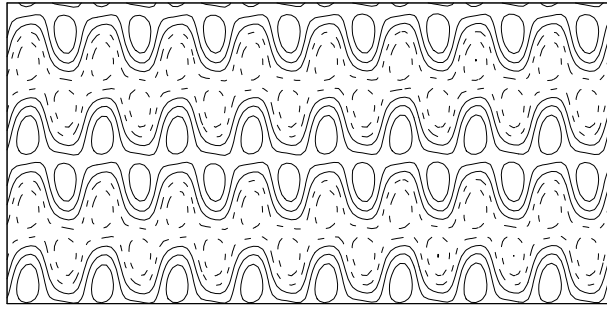


Figure 2: Geopotential at the surface for the most unstable mode when the amplitude of the primary wave is 25 mb, obtained with a long integration from random-noise initial condition. The domain length is 28,000 km and contains 8 primary wavelengths.

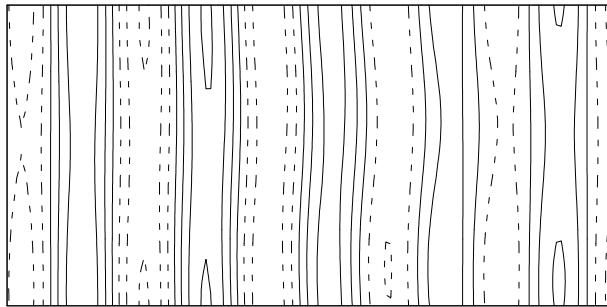


Figure 3: Same as Fig.2 but for primary wave amplitude of 1 mb.

linearly with the amplitude of the primary wave, and the spatial structure is that of 'frontal' baroclinic waves that are growing on the thermal gradient associated with the primary wave itself, rather than the mean north-south gradient. The modes appear to be locked in phase with the primary wave, and their phase speed is that of the primary wave itself, lower than the midlevel wind (see Fig. 1).

3 OROGRAPHIC PERTURBATION

In Fig.4 we show the evolution of the orographic perturbation generated when a primary Eady wave 3500 km long and 25 mb deep encounters a gaussian mountain with 1000 km half-width in all directions. The mountain's height is 500 meters but the same result would have been obtained with any other height, as the model is linear and the topography is represented as a lower boundary condition at $z=0$, although the dimensional time scale of the development does depend on the slope of the mountain. Comparison with Fig.5, which displays results for a primary wave of small amplitude, reveals differences in the path of the orographic perturbations, that are generated on the upwind side

and advected by the wind, which in the large amplitude case is not just zonal but the sum of zonal and eddy. The same behavior was shown in Fantini and Davolio (2000) for the semigeostrophic version of this model, whose results, apart from the contraction of the areas of positive vorticity due to the coordinate transformation, are essentially the same as presented here. The difference in propagation properties can be described locally as advection of the orographic perturbation by different basic winds, or globally as a projection of the orographic disturbance on normal modes with different spatial structures, as shown in Figs 2 and 3.

The mode excited by the mountain in the small amplitude case is not actually the one shown in Fig.3 but the one with a node at the latitude of the mountain's peak, as can more easily be seen in Figs 6 and 7, which compare the orographic perturbations in the two cases of small and large amplitude of the primary wave, at a later time than shown in Figs 4 and 5, and with a wider spatial view.

4 ABSOLUTE AND CONVECTIVE

An interesting characteristic of the orographic perturbation in the large amplitude case is the persistence of the perturbation wave packet generated by the mountain near the mountain itself, despite the positive phase speed of the individual components. This behavior can better be seen in Fig. 8, which is a time-longitude plot of the geopotential perturbation at the surface, at the latitude of the mountain's centre. The left panel shows the actual perturbation, which is periodically reduced by a factor of 1,000 when it becomes too large for numerical stability (since the model is linearized there is no equilibration at finite amplitude for the perturbation). In the right panel the perturbation normalized with its maximum value at each time is shown, to give a better representation of the movement of the individual elements of the packet compared with the packet as a whole.

The above 'absolute' character of the instability in the large amplitude case is contrasted with the 'convective' behavior of the small amplitude case, when the perturbation wave packet moves with the same speed as the individual modes, as can be seen in Fig.9, which gives the same time-longitude plot the orographic perturbation induced by a 1 mb-deep primary wave. It can clearly be seen that although the orographic perturbation is continuously recreated by the interaction of the primary wave with the mountain, the growing wave packet moves away from the mountain. A more detailed presentation of this point can be found in Fantini and Davolio (2000b).

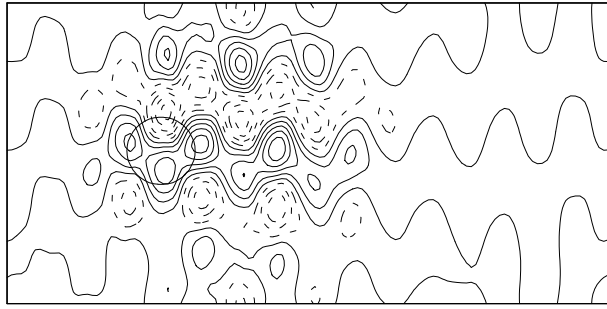


Figure 6: Orographic perturbation at the surface in the case of primary wave 25 mb deep, at 140 hours after initialization. The whole 28,000 km domain is shown.

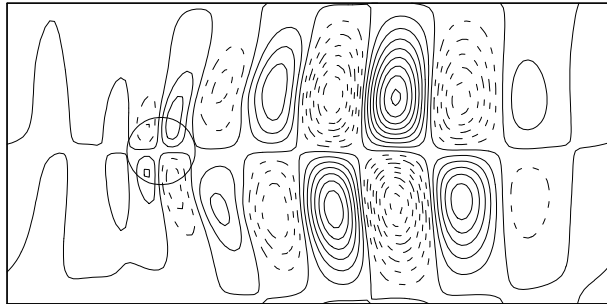


Figure 7: Same as Fig.6 but at 380 hours, for 1 mb deep primary wave.

5 DISCUSSION

This study was set up with the intent to examine the interaction of a front with an isolated mountain. In this idealization the front is represented by the thermal gradient associated with an Eady wave of finite amplitude. It would be possible (see Fantini and Davolio, 2000) to apply the semigeostrophic coordinate transformation to the present results to obtain a more realistic frontal structure, but the nonlinearity of the transformation would also confuse the study of the linear stability properties of finite amplitude Eady waves, which shows here a transition from a 'convective' to an 'absolute' behavior of the orographically generated wave packet when the amplitude of the primary wave is large enough (around 10 mb for the dimensional parameters used here).

It is fairly obvious that the large scale propagation properties of the orographic perturbations are not adequately represented by an f -plane (consider e.g. the size of the domain shown in Figs 6 and 7), and that a more realistic geometry would be needed in that regard, together with a better representation of the finite size of the mountain (e.g. terrain-following coordinates). The local structure of the orographic perturbations seems reasonably represented on the scale of Figs 4 and 5,

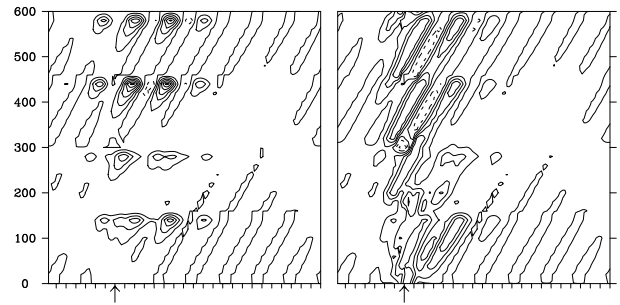


Figure 8: Time-longitude plot of the surface geopotential perturbation at the latitude of the mountain's peak, for the case of a 25 mb-deep primary wave. Time (on the ordinate) is in hours, and the marks on the horizontal axis are spaced by 1,000 km. The arrow on the bottom indicates the location of the mountain's center. Left: Dimensional orographic perturbation, which has been subject to periodic amplitude reduction to preserve numerical stability during the model integration. Right: Orographic perturbation normalized with its maximum at each time.

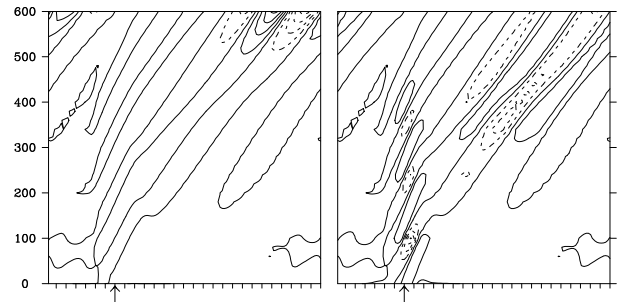


Figure 9: Same as Fig.8 but for the 1 mb case.

and it would be important to know at which stage of the evolution the nonlinear terms here disregarded would change the behavior of the orographic perturbation. Equally important are the modifications that the consideration of an unstable primary wave, or one that has reached nonlinear equilibration, would bring to the results presented here. All of the above points will be taken into account in future developments of this study.

References

- Fantini, M and S. Davolio, 2000: Formulation of a semi-geostrophic model of frontal interaction with isolated orography. *Meteor. Atmos. Phys.*, **72**, 261–270.
- Fantini, M and S. Davolio, 2000b: Instability of Neutral Eady Waves. *J. Atmos. Sci.*, **submitted**.
- Pierrehumbert, R. T. and K. L. Swanson, 1995: Baroclinic Instability. *Ann. Rev. Fluid Mech.*, **27**, 419–467.

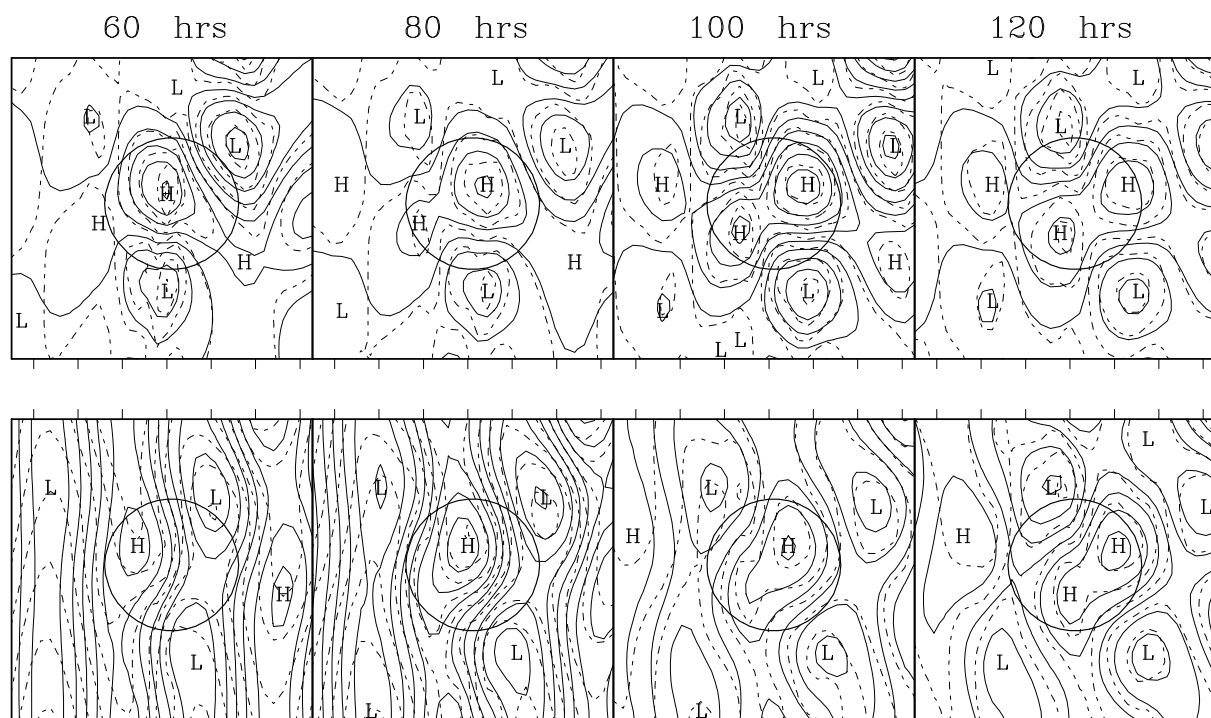


Figure 4: Time evolution of the perturbation generated by interaction of a primary wave 25 mb deep with a gaussian mountain 500 m high. The 50 m orographic contour is shown. Upper: Perturbation geopotential (solid line) and potential temperature (dashed) at the surface. Lower: Total (Primary wave plus Orographic perturbation). The marks on the boundaries are 1,000 km apart.

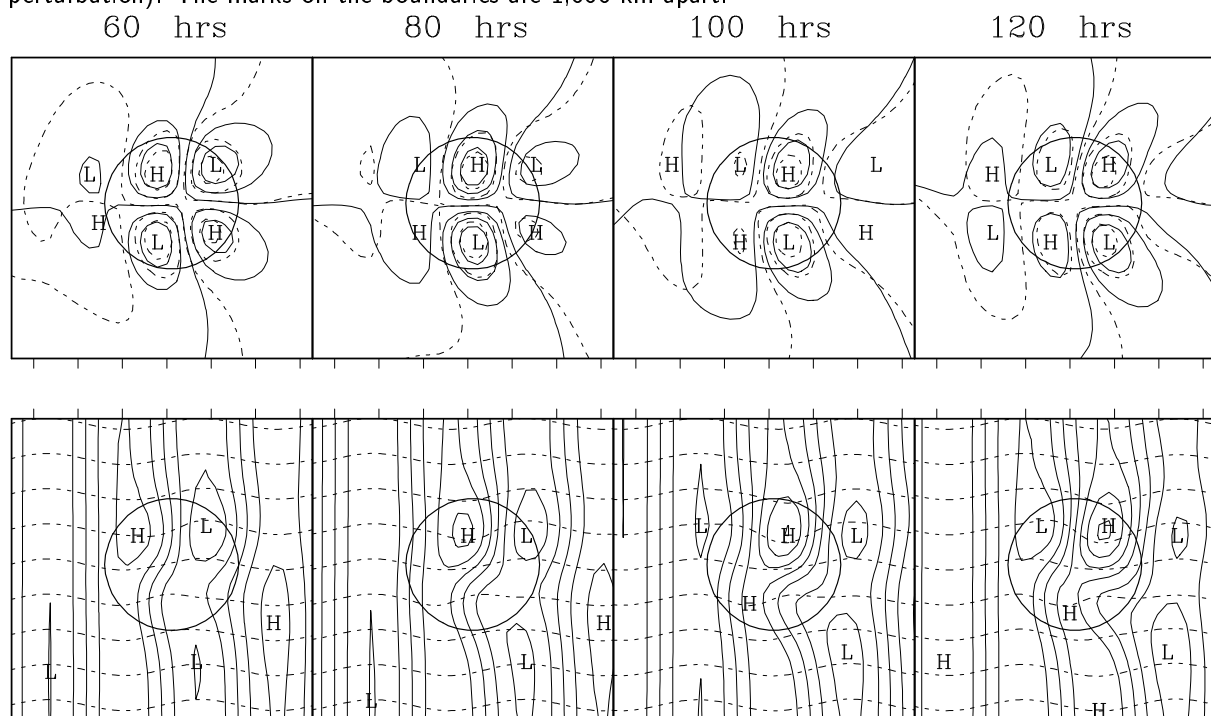


Figure 5: Same as Fig.4 but for a primary wave amplitude of 1 mb.